2014

A Diagnosis Feature Space for Condition Monitoring and Fault Diagnosis of Ball Bearings

Ali Kahirdeh
Louisiana State University and Agricultural and Mechanical College, kahirdeh.ali@gmail.com

A DIAGNOSIS FEATURE SPACE FOR CONDITION MONITORING AND FAULT DIAGNOSIS OF BALL BEARINGS

A Thesis

Submitted to the Graduate Faculty of the
Louisiana State University and
Agricultural and Mechanical College
in partial fulfillment of the
requirements for the degree of
Master of Science

in

The Department of Electrical Engineering and Computer Science

by
Ali Kahirdeh
B.Sc., Isfahan University of Technology, 2005
M.Sc., Iran University of Science and Technology, 2007
December 2014

To my parents, Manouchehr and Mohtaram,

My sisters, Pegah and Baharak, and my lovely wife, Hila

Acknowledgements

I would like to thank my advisor Professor Dr. Kemin Zhou for his constant support and guidance throughout this study. I am also thankful to my committee members Dr. Gu, and Dr. Wei.

Table of Contents

Abstract

The problem of fault diagnosis and condition monitoring of ball bearings is a multidisciplinary subject. It involves research subjects from diverse disciplines of mechanical engineering, electrical engineering and in particular signal processing. In the first step, one should identify the correct method of investigation. The methods of investigation for condition monitoring of ball bearings include acoustic emission measurements, temperature monitoring, electrical current monitoring, debris analysis and vibration signal analysis. In this thesis the vibration signal analysis is employed. Once the method of analysis is selected, then features sensitive to faults should be calculated from the signal. While some of the features may be useful for condition monitoring, some of the calculated features might be extra and may not be helpful. Therefore, a feature reduction module should be employed. Initially, six features are selected as a candidate for the diagnosis feature space. After analyzing the trend of the features, it was concluded that three of the features are not appropriate for fault diagnosis. In this thesis, two problem is investigated. First the problem of identifying the effects of the fault size on the vibration signal is investigated. Also the performance of the feature space is tested in distinguishing the healthy ball bearings from the defective vibration signals.

Chapter 1. Introduction and Literature Review

1.1 Methods of Condition Monitoring and Fault Diagnosis

Rotating machineries play a vital role in various industries. Unexpected breakdowns of those machineries increase the cost of production and manufacturing lines. The failure in rotary machines are mostly due to failure of the components. One of these components that cause major problem are ball bearings. Therefore, preventive methods should be employed in order to monitor the performance of the ball bearings.

In this thesis, the vibration signals of ball bearings will be studied in order to define a feature space for the fault diagnosis purpose. The fault diagnosis programs usually contains main steps of: signal measurement, feature extraction, and feature reduction and pattern recognition. One problem for the pattern recognition module is that the feature space is usually complicated and there are extra features. In order to have a better performance, proper feature reduction module has to be employed.

The goal of this thesis is to define a feature space that does not require a redundancy reduction module. Such feature space facilitates the performance of a typical automatic fault diagnosis system. In order to accomplish this goal, several features will be studied out of which three will be selected as the diagnosis feature space. In this thesis, signals of a ball bearing with an inner race way fault is selected and compared with a base signal of a healthy ball bearing.

The purpose of maintenance method is to diagnose the faults and the broken components and to reduce the down time of the machinery. The cost of maintenance in United States exceeds the amount of a trillion dollars yearly. The dated and ineffective methods of maintenance also increase the cost of the operations of the plants. There are several methods of plant maintenance that can be categorized as following:

1. Run to failure methods

2. Preventive maintenance

3. Predictive maintenance

The first method which is the most expensive method used, lets the component operate until a failure occurs. This method is rarely used in the industries anymore. The second method inspects the machinery after a certain period of time in order to reduce the possible failures in operation. The time intervals of the operation is decided based on the performance of the machinery. This method is mostly employed for machineries whose safety level are critical. The total cost of such maintenance strategies is still high and undesirable. In the predictive maintenance the decision is made based on the current state of the machinery. The procedure is that the machinery is equipped with a number of different sensors that monitor the condition of the equipment. The sensors can be of different types and measure various response of the machinery. For example, Infrared camera can measure the temperature of the equipment and its thermal response during the operation. Accelerometers can be utilized to measure the vibration pattern of the machinery. Acoustic emission sensors can also measure the acoustic characteristics of the machinery. By employing such sensing systems for the equipment in a predictive maintenance method, the detection of the faults can be realized as they occur.

Research shows that ball bearings are one of the most common sources of failure in rotating machinery. For example, in the case of the induction motors the distribution of the faults shows that 41 percent of the common failures belongs to ball bearings while 37 percent belong to stator faults, 10 percent is related to rotor faults and 12 percent is related to the other faults [1].

Also in the failure mode analysis of the generators of the wind turbines, it has been shown that in the medium generators, 70 percent of the faults are related to the bearings and in the large

generators, 50 percent of the faults corresponds to bearings. Figure 1.1 depicts the distribution of the faults in the example of the wind turbine generators [2].

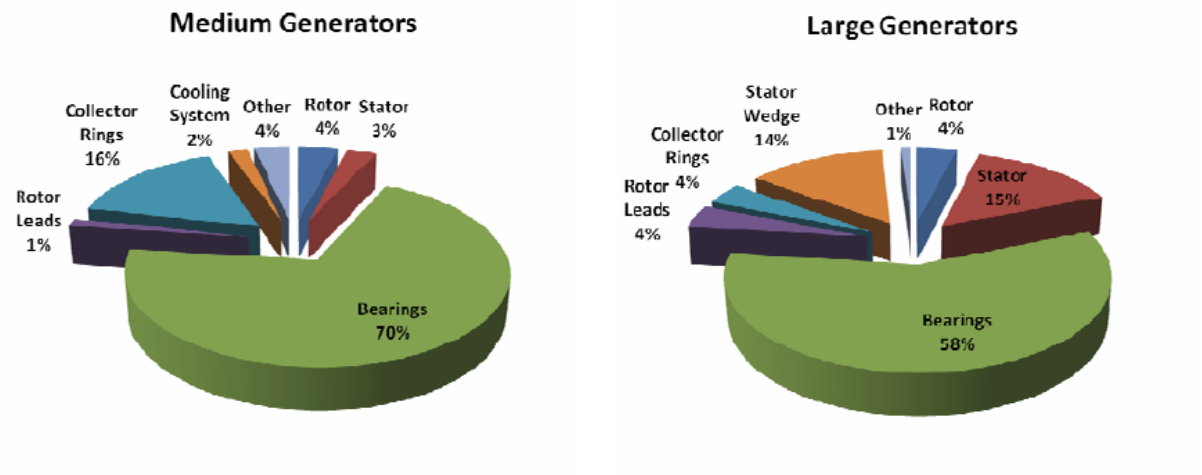

Figure 1.1. The distribution of the faults in the wind turbine generators [2].

A ball bearing can be regarded as a complex system that is made of two raceways, the so-called inner and outer ring, and a set of rolling elements that roll between the two raceways. For different types of the ball bearings the rolling element may differ in shape and size. For example different shape of the rolling elements makes different types of bearing that are suitable for various applications. These rolling elements could be of the form of balls, cylindrical rollers, and tapered rollers as depicted in Figure 1.2.

Ball bearings are widely used in a variety of industries and machineries such as electric motors, pumps and power transmission systems. Ball bearings has this advantage that they have less power loss and frictional heat generation comparing to hydrodynamic bearings. They also require small amount of lubrication for satisfactory operation [3]. There are several mechanisms for the failure of a ball bearing. The failure can be due to mechanical damage, wear damage, lubricant deficiency, cracking and corrosion damage. The mechanical damage can be created due to overloading. The damage due to overload is called brinelling and can be diagnosed by noisy operation of the

bearings. This type of damage can happen in bearings that are subjected to vibration loads during the transit. The other type of failure that can occur is wear that results in loss of clearance and dimension in ball bearings. Also as a result of wear, lubricant contamination can occur. At the points where wear appears stress increases and may cause crack initiation.

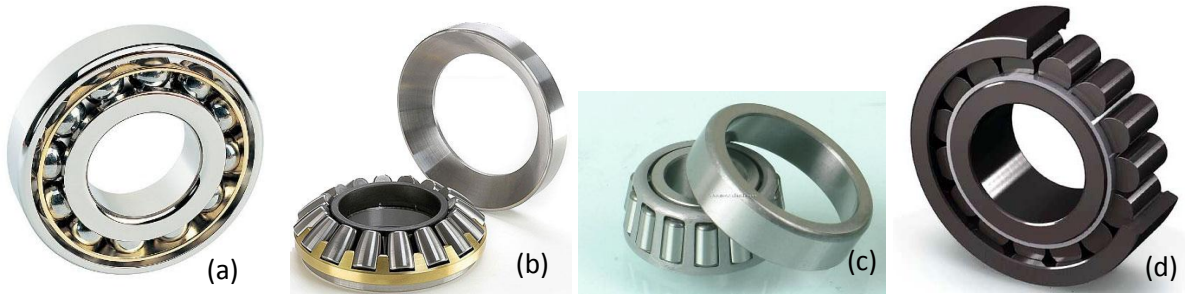

Figure 1.2. Various types of ball bearing. a) Ball bearing, b) Roller thrust bearing, c) Tapered roller bearing, d) Roller bearing.

The surface of the raceways also undergo progressive contact deteriorations as a result of improper lubrication. Lack of adequate lubrication in ball bearings also result in temperature rise in the loading area. In such conditions the failure in the surface of the bearing is accelerated. This is visible from the changes in the surface color. The crack damage in bearings can occur due to excessive stress concentration. Two of the reasons for crack initiation are fatigue and overload.

There is another mechanism of damage called corrosion damage. This types of damage usually happens in bearings that are subjected to environments where lubricants are mixed with corrosive substances. The mix causes surface oxidation and produce particles. Such particles can cause an abrasive type of wear on the surface. The worn surface can be also the sites of stress concentration from which spalling initiates. Appearance of the surface defects on the raceways of the ball bearings increases the vibration level of the ball bearings. A variety of defects can appear on the elements of a ball bearing, such as spalling, pits and lack of the alignment in the ball bearing. Irrespective of the type of the defect in the ball bearing, the resulting vibration can be detected by a transducer. The measured signal then should be analyzed using signal processing methods to

reveal the information related to the damage. Vibration of the machineries is an indicative of the health of them and is a more effective method in detecting the faults of the rotating machineries comparing to other non-destructive tests. It is also a cost-effective method in fault diagnosis that can be performed by means of simple sensors and instrumentations. The vibration data can be also measured using portable devices and for continuous monitoring purpose may be installed for critical systems. Typically, the instrumentation required for measuring the vibration signals contains data acquisition unit, signal conditioning device and data storage equipment. There is also a progressive demand for automatic fault diagnosis systems where the task of the diagnosis is performed intelligently by means of an intelligent algorithm.

Fault detection and diagnosis is a hierarchical and multistep procedure. Different steps in an automatic fault diagnosis system is: signal measurement and data acquisition, signal processing, feature extraction, feature reduction, pattern recognition and classification. These steps are shown in Figure 1.3, respectively. In the first step, the physical measurement is performed and the system response is measured using vibration signal, acoustic, thermal or any other meaningful signal. Afterwards, feature extraction is performed using appropriate signal processing and post processing technique.

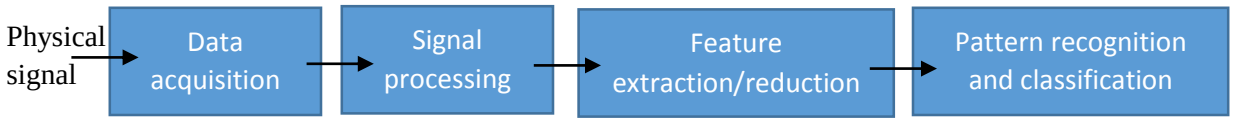

Figure 1.3. The modular schematic an automatic fault diagnosis system.

The signal processing can be performed in different domains such as time domain, frequency domain, time-frequency or time-scale domain. In fact, this step is a mapping from the raw signal into a feature space. Conventional approaches in fault diagnosis are based on expert's interpretation of the features to identify the faults information from the feature space. But, this is

a time-consuming procedure and can be inefficient in particular when multiple features are employed for the diagnosis feature space.

Automatic fault diagnosis methods is employed to tackle this problem. In signal processing step of the automatic fault diagnosis systems several methods has been employed in the literature. For example, Heng *et al.* [4], performed statistical analysis on the time domain vibration signal. They studied crest factor and statistical moments such as kurtosis and skewness. It was concluded that the statistical moments are affected by shaft speed. Other statistical features such as Kolomogorov-Smirnov (KS) statistic is employed by Kar *et al.* [5]. This statistical signal processing technique is performed to investigate if two signals have the same distributions. The KS statistics is also utilized in the analysis of the acoustic emission (AE) signals of a rotor-stator rub by Hall *et al.* [6]. In their study, the cumulative distribution function of the measured AE signals is modeled with respect to the theoretical distributions and the KS statistics is employed as a diagnosis feature. A ball bearing is diagnosed as faulty if the time domain feature exceeds a threshold. However, the accurate definition of the threshold is a difficult task and dependent on the application under investigation. Other than time domain signal analysis, the frequency analysis is also a popular task in signal processing of the vibration signals. One of the main advantages of the frequency analysis over time domain signal analysis is that it makes possible to isolate the frequency components that contains the faults information from the rest of the frequency content. The analysis in the frequency domain can be based on identifying the characteristics frequencies in the spectrum of the vibration signal and studying the evolution of the amplitude of the characteristics frequencies in the frequency domain. Signal enhancements is also performed in frequency domain using cepstrum analysis in the research performed by Choi *et al.* [7]. In their work by minimizing the signal power the cepstrum representation of the signal, the faulty signals are detected in a noisy environment.

The fault signals are usually of non-stationary nature. Therefore, more sophisticated methods are required than frequency domain analysis. In this regards non-stationary signal analysis is employed using time-frequency and time-scale signal analysis. Time-frequency signal analysis is a technique that study the signal in both time and frequency domain simultaneously utilizing a time-frequency distribution (TFD). Time-scale analysis is similar to TFD but it should be noticed that the signal representation is in two-dimensional space of time and scale where the scale axis has a specified relation with time. In the application of the time-frequency analysis Gabor transform [8, 9] is used to interpret the acoustic vibration signals where the information acquired from the sensors is represented in the form of time-varying parameters of dominant signal frequency, the breadth of the frequency content and its effective energy [10]. Short Time Fourier Transform (STFT) is also applied by Cocconcelli *et al.* [11] on the vibration signals measured from AC brushless motors and it was shown that the sum of STFT coefficients is used as indicator of the damage. In their study, the STFT for each cycle is averaged in the time-frequency domain in order to enhance the fault signature [11]. The application of the wavelet transform and time-frequency analysis has been around a number of main aspects including: time-frequency analysis of the signals, the fault feature extraction, the singularity detection of the signals noise elimination and extracting the weak signals, compression of the vibration signals and system identification. One of the first works in time-frequency signal analysis, is the work by Wang and Mcfadden [12] where they benefitted from the multi-resolutions characteristics of the wavelets to display all possible types of the gear faults by a single time-scale distribution resulting from the transform. Dalpiaz *et al.* [13] also employed wavelet transform for monitoring a pair of gears affected by fatigue cracks and concluded that the wavelet transform is a good tool for crack detection and its effectiveness is increased if the residual part of the time-synchronous averaged signal is processed. The application

of the time-frequency or time-scale signal analysis is not limited to diagnosis of bearings and gears. The cracks in rotors and structures is also investigated using wavelet transform. Scalograms and space-scale energy distribution of the discrete wavelet transform of measured vibration signals is shown to detect the transverse propagating crack of an overhang rotor [14]. Peng *et al.* [15] were able to able to identify the faults at early stage. In their study, the rotor to stator rub, oil whirl and coupling misalignment of a power generator unit is analyzed using a scalogram. In the application of the wavelet transform as a feature extraction method, Chen et al. [16] utilized multi-scale wavelet analysis to determine the singularity of the transient vibration signal. In their study, after decomposition of the transient signals, the wavelet coefficients are used as a fault feature. Similar analysis is performed by Yen and Lin [17] and Goumas et al. [18] who used the wavelet coefficients as fault features.

Another way of employing the wavelet transform is to use it for singularity detection. Singualr points includes peaks, the discontinuities and etc. A standard method of singularity detection is the method of wavelet modulus maxima introduced by Mallat [19]. Sun *et al*. [20] used a singularity analysis across all scales of the continuous wavelet transform and could identify the location of the defect induced bursts in vibration signals.

In fault diagnosis and condition monitoring, one of the most important steps are denoising and extraction of the weak signals. Altman [21] enhanced the detection and diagnosis of low speed rolling element bearings using a discrete wavelet packet analysis. Lin *et al*. [22] used a wavelet based method to increase the signal noise to ratio in signals measured from machinery sound.

In an automatic fault diagnosis system, a unit of data reduction is required. Since in signal processing module usually the number of extracted features is higher than what is needed. Therefore, redundancy reduction is usually performed. One of other reasons to perform a

redundancy reduction analysis is that the sensitivity of various features that are indicators of machine health can vary under different operating conditions and therefore, a feature selection method is needed.

Malhi et al. [23] presented a feature selection method based on principal component analysis (PCA) to choose the most representative features for defect classification and the method was reported as an effective tool for machine health assessment.

He *et al*. [24] also employed PCA as a nonlinear feature extraction method. A kernel PCA was successfully employed to build a two dimensional feature space from multidimensional feature space formed by time domain and frequency domain features. Akbaryan [25] also employed PCA analysis to reduce the size of the feature space. In their study, the wavelet coordinate is projected to a lower dimensional space where the correlation among the new space variables are minimized [25]. After preparing the feature space and applying the redundancy reduction techniques, pattern recognition and classification is usually applied on the feature space. In order to automate the process of condition monitoring, Ghate *et al.*[26] employed a multi-layer perceptron (MLP) neural network as a classifier. The method provide an inexpensive and reliable method for fault diagnosis. Statistical parameters are used as the feature space and its dimension is reduced using PCA. Lei *et al.* [27] used wavelet transform (WPT) and empirical mode decomposition to define characteristics information of the faults and preprocess the vibration data. A combined feature set containing the time domain feature extracted from the original vibration signals as well as the preprocessed signals are then input to a radial basis function (RBF) network to identify different machine operating conditions. An advantage of using neural network in fault diagnosis systems is that neural classifiers are robust against noise.

Other than neural networks, approaches such as fuzzy logic, clustering approaches and support vector machines also are utilized for machine health assessment. An adaptive neural fuzzy inference system was trained by Lou [28] as a diagnostic classifier. The neuro-fuzzy classification is applied on the feature vectors created by wavelet transform.

1.2 Problem Statement and Current Issues

Through an extensive literature review of the methods of fault diagnosis of rolling element bearings, it was shown that the literature contains a large number of features of the vibration signals that has been studied in identifying the faults. The common method to automate the procedure is that firstly a large number of features are selected and then using principal component analysis (PCA), three first PCs are chosen as a diagnosis feature space. The selected PCs are the inputs to the pattern recognition module for classification purpose. This procedure is popular since the two-dimensional or three-dimensional representation of the feature space is highly desirable and it can be easily interpreted. However, this method has certain problems. First, the output of the feature reduction module is often hard to interpret and the reduced space usually does not have any physical meaning. One of the main problems in using PCA is that since the features are mostly of different scales, the variables with high absolute variance will dominate the first principal component. Additionally, the feature space is complicated and drawing the two-dimensional and three-dimensional decision boundaries is often a complicated task.

The goal of this thesis is to investigate new features for the fault diagnosis of the ball bearings. These features are chosen from a variety of domains such as statistical features, time domain features and time-frequency features. Finally a new feature space is introduced as a diagnosis feature space. The procedure to obtain the new diagnosis feature space is depicted in Figure 1.4.

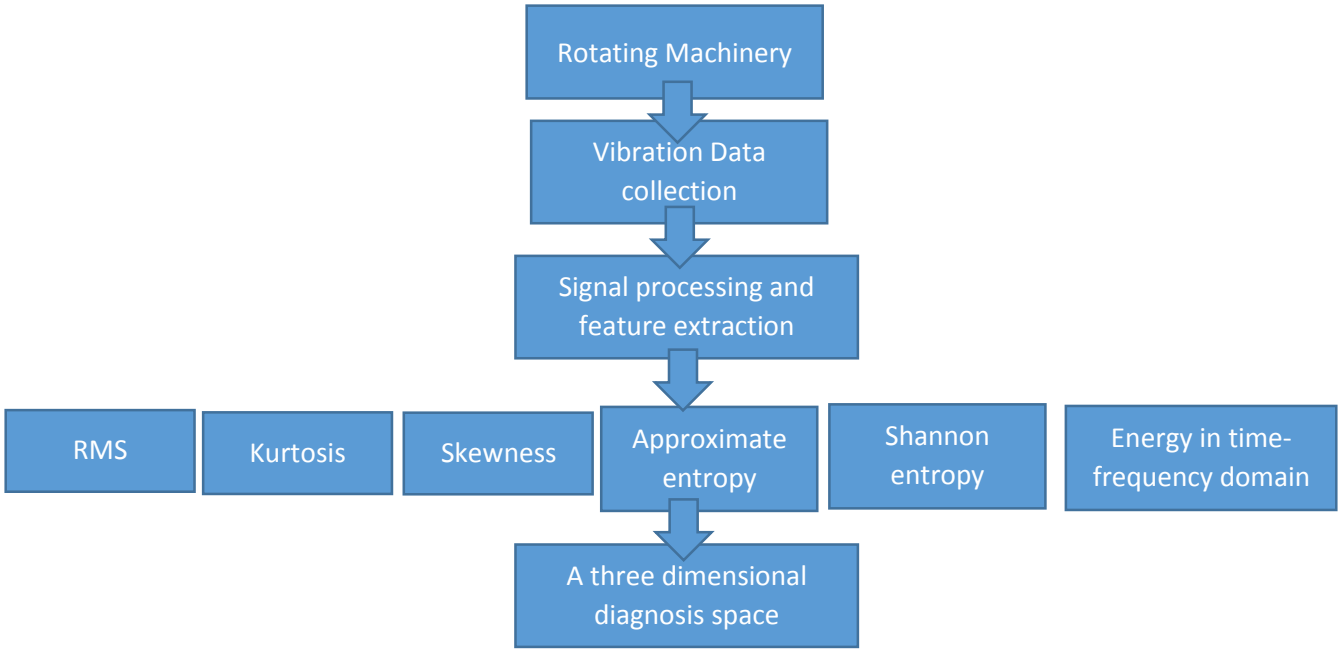

Figure 1.4. The procedure to obtain a diagnosis feature space.

Chapter 2. Vibration Signal Analysis

2.1 Condition Monitoring and Fault Diagnosis

Rolling element bearings are critical components in most of the machineries and failure in these parts may cause catastrophic incidents. The defects of the ball bearing can be created as early as during the manufacturing or due to fatigue and cyclic loading. Therefore, condition based maintenance (CBM) techniques must be used to avoid any unexpected failure and break down. The CBM is a method which offers maintenance decision based on the data gathered during the operation.

Various methods are used for data collection. The available methods that are used are such as: vibration analysis, temperature measurement, and wear debris analysis. Vibration analysis is the most widely used method for condition monitoring. Recently, with the availability of the sophisticated data acquisition systems, acoustic emission signals can also be measured from the ball bearings. The procedure consists of three main steps: data acquisition, data processing and decision making. Several methods can be applied to the vibration data to identify the meaningful data. These methods are vibration measurements in time, frequency, and time-frequency domain, the shock pulse method and wavelet analysis. The sources of vibration and noise in ball bearings are due to several reasons:

1. The imperfection in the geometry which results in random shock
2. Changes in the stiffness of the ball bearing
3. Surface defects that once the bearing is loaded causes vibration

The defects can also be categorized into two groups of the distributed defects and the localized defects. The distributed defects are due to manufacturing malfunctions and surface roughness variation. The localized defects contains faults due to cracking and fatigue failure. Once the defects

interact with other elements of the ball bearing such as balls, the sudden surface changes causes a shock wave that can be monitored to identify the fault of the bearing. To conduct a series of experimental studies on the ball bearing, two approaches exist. The first is to let the ball bearing operate on its own until it fails under normal conditions. But this is a very time consuming method and will not yield to results within a reasonable time frame. The second method is to introduce the defects on the elements of the ball bearing artificially using an abrasive tool or electro discharge machining (EDM). One may also remove the lubrications or increase the load above the operating guidelines to create the defect. The size of the defects can be varied also in order to simulate different sizes of the defect.

2.2 Feature Extraction in Time and Time-Frequency Domain

In this section the features calculated from vibration signals are briefly introduced.

2.2.1 RMS in time domain

The RMS (root mean square) value of the vibration signal is the normalized second statistical moment of the signal as defined by equation 1.

$$RMS = \sqrt{\int_0^T \frac{1}{T}(x(t) - \bar{x})^2 dt} \quad (1)$$

where T is the length of the time record used for the signal and $\bar{x}$ is the mean value of the signal as defined below.

$$\bar{x}(t) = \frac{1}{T}\int_0^T x(t)dt \quad (2)$$

The RMS of a signal is commonly used to describe the steady state of a time varying signal. The RMS is the simplest method to measure the overall level of the vibration of the ball bearing.

2.2.2 Crest factor

Another factor used as a health indicator can be obtained if one divide the peak level of the vibration data to the RMS value as in equation 3. The new feature is defined as crest factor.

$$Crest\ factor = \frac{Peak\ value}{RMS} \quad (3)$$

The RMS feature has been used in several studies including Mathew et.al. [29]. Figure 2.1 shows the effect of the damage on the several features including the RMS value, peak level, RMS times kurtosis level, standard deviation, arithmetic mean and geometric mean of the acceleration data. The evolution of these features with respect to time depicts a similar pattern meaning that one of the features can be used as a health indicator.

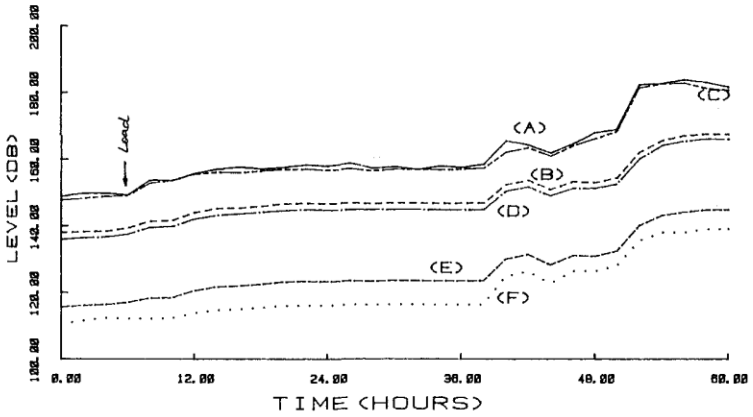

Figure 2.1. Time domain features over the course of one experiment. RMS level in vibration changes with level of the damage [29].

2.2.3 Probability density function

Another feature is the probability density function of the acceleration signal. It is reported that a healthy ball bearing shows a Gaussian probability density function. The shape of the probability density function deviates from Gaussian, once the faults appear. Figure 2.2 shows the probability density function for a bearing in good condition with a superimposed Gaussian curve. Figure 2.2b shows the same data with a logarithmic probability scale. Appearance of damage in bearing, results in change in probability density function. Higher values of acceleration signal results in the changes of the tales of the probability distribution. Such changes are shown, in Figure 2.3.

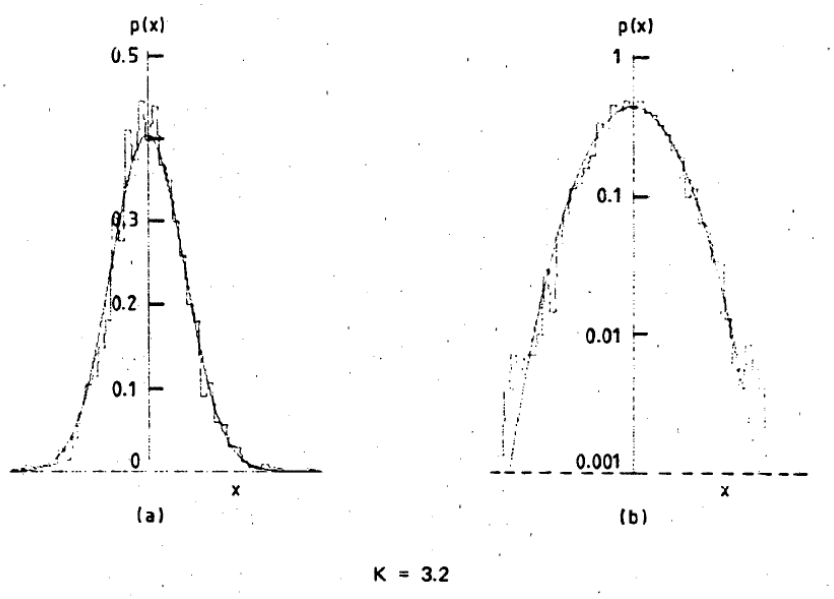

Figure 2.2. Probability density function of a healthy bearing [30].

One can also study the statistical moments of the probability density function to obtain a descriptive feature. The moments are defined as following:

$$M = \int_{-\infty}^{+\infty} x^{-n} P(x) dx \;\; n = 1,2,3, \dots m \qquad (4)$$

where $p(x)$ is the probability density function of the variable x.

While the first moment is known as mean and the second moment is recognized as variance, the third moment if normalized with standard deviation to the power of three is known as skewness. Also the fourth moment normalized with respect to the standard deviation to the power of four is called kurtosis.

2.2.4 Skewness

Skewness is a statistical measure to determine if a distribution of the data is asymmetry around its sample mean. This measures attains both positive and negative values. If it is negative, it means that the tail of the probability density function in the left side is longer than the tail of the distribution in the right side. If skewness is positive, it means that the tail of the probability density function in the right side of the distribution is longer than its left side.

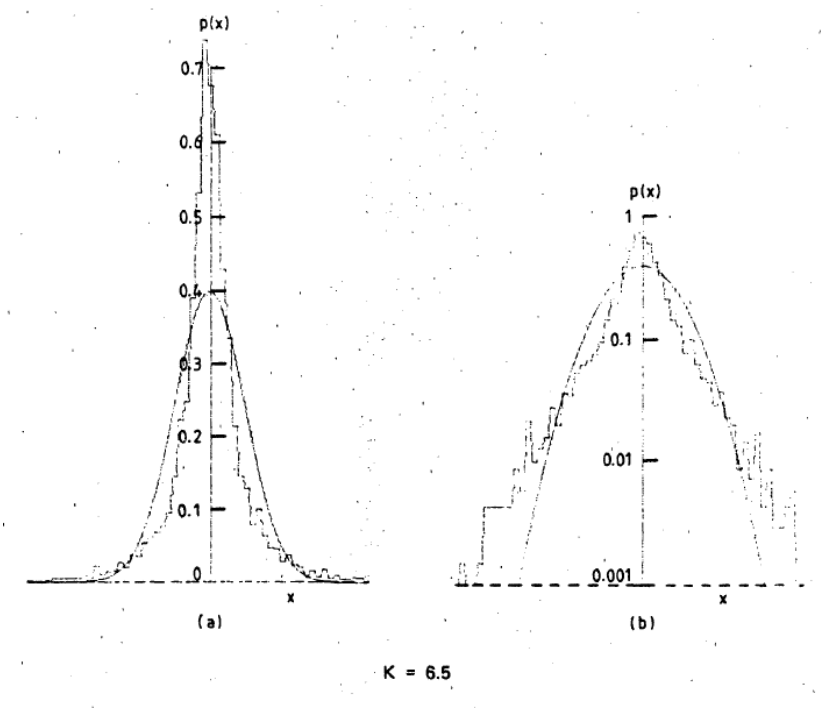

Figure 2.3. Probability density function of a damaged bearing [30].

The skewness for a perfectly symmetric distribution is zero. The following formula was used for computation of skewness.

$$k = \frac{E(x-\mu)^3}{\sigma^3} \tag{5}$$

where μ is the mean of x, σ is the standard deviation of x, and E (t) represents the expected value of the quantity *t*.

2.2.5 Kurtosis

Kurtosis is a measure to describe the shape of the distribution. It represent how outlier-prone a distribution is. In the application of the signal processing, kurtosis can reveal the flatness or the spikiness of the signal. Its value is very low for good bearing and high for bearings due to spiky nature of the signal. The mathematical definition of the kurtosis is provided in eq. 6.

$$k = \frac{E(x-\mu)^4}{\sigma^4} \tag{6}$$

where μ is the mean of x, σ is the standard deviation of x, and E(t) represents the expected value of the quantity t.

Figure 2.4 shows the kurtosis level of a typical experiment on a failed ball bearing. The kurtosis level shows an increase around 950 hours after the start of the test. Initial values of the kurtosis is around 3 and then it increase to higher values [31]. The kurtosis value for a signal of Gaussian distribution is around 3. But as the faults appear on the ball bearing and the signal becomes noisy the distribution changes from Gaussian and kurtosis feature values higher than 3.

2.3 Features in Frequency Domain

Other than time domain signal analysis, frequency domain analysis is also one of the most widely used methods in the ball bearing analysis. In frequency domain analysis, both low and high frequency range of the signal is analyzed employing FFT analyzers. Due to complexities in the vibration behavior of the ball bearing both ranges of the frequency is important to be studied.

The interaction between the defects and the rolling elements causes shock pulses that excites the natural frequency of the whole system including, ball bearing elements, housing and structure. This results in an increase of the vibrational energy at these excited frequencies. These resonance frequencies can be calculated theoretically. Each bearing has a characteristic frequency. A defective bearing has an increased vibrational energy at these frequencies.

Equation 7-10 shows the characteristics frequencies for outer bearing race fault, inner bearing race faults, ball fault and cage faults, respectively.

$$f = \left(\frac{n}{2}\right) f_r \left[1 - \frac{b_d \cos(\beta)}{d_p}\right] \tag{7}$$

$$f = \left(\frac{N}{2}\right) f_r [1 + b_d \cos(\beta)] \tag{8}$$

$$f = \frac{d_p f}{2 b_d} \left\{1 - \left[\frac{b_d \cos(\beta)}{d_p}\right]^2\right\} \tag{9}$$

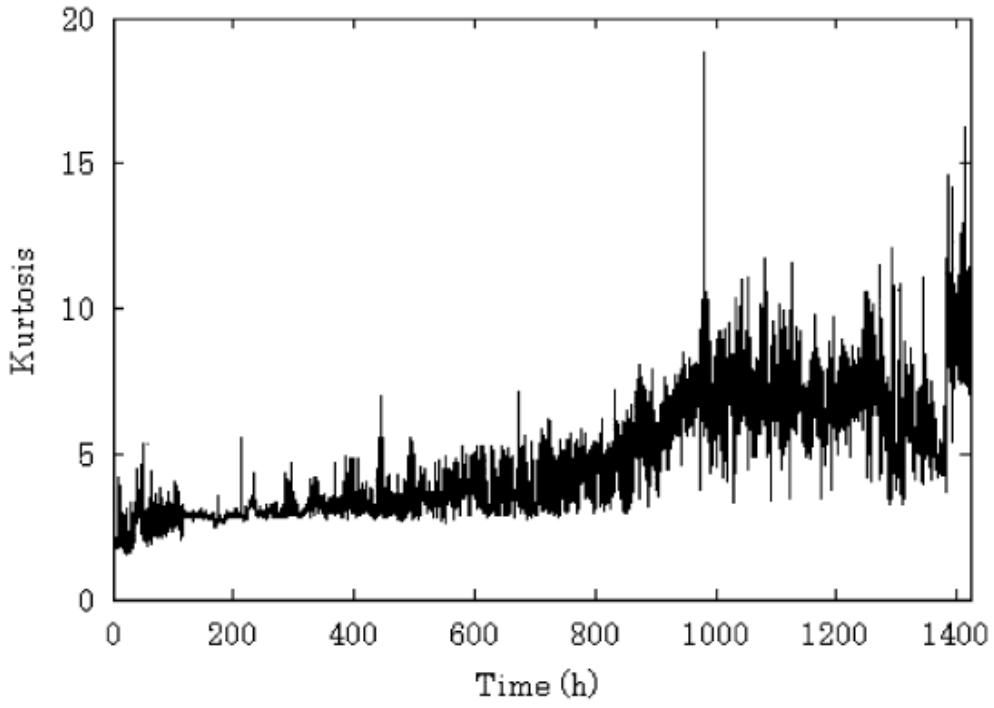

Figure 2.4. The kurtosis history of the ball bearing vibration [31].

$$f = \left(\frac{f_r}{2}\right)\left[1 - \frac{b_d \cos(\beta)}{d_p}\right] \tag{10}$$

where f_r is the rotational frequency, N is the number of balls, b_d and d_p are ball diameter and pitch diameter and β is the contact angle of the ball with the races [32]. Figure 2.5 shows a comparison between the frequency spectrum of a damaged bearing (B) and a healthy bearing (A). As it can be observed the vibration level in the damage bearing is higher than that of the healthy bearing in all of the frequency ranges.

Karacay et.al. [31] performed a long duration experiment on a ball bearing testing system and measured the spectrum at two different time related to two different stage of health of the ball bearing. Figure 2.6 shows the spectrum of the vibration of the ball bearing after 130 hours of operation where peak to peak and RMS values are stable. The dominant peaks at spectrum are at

shaft speed and its harmonics (53 and 106 Hz). Peak at the ball passage frequency is also present in the spectrum at frequency of 190 Hz [31].

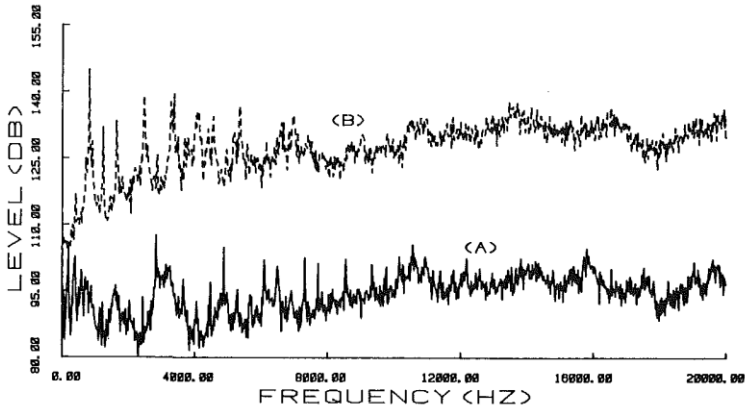

Figure 2.5. Comparison between the frequency spectrum of the damage bearing and healthy bearing [29].

While Figure 2.6 shows the spectrum of the ball bearing in its healthy stage and after almost 130 hours of operation, Figure 2.7 shows the spectrum of the ball bearing at its damaged phase and after almost 980 hours of operations. Although the dominant frequencies are around the shaft speed, the faults frequencies related to ball pass frequency, inner race frequency also exist in the spectrum.

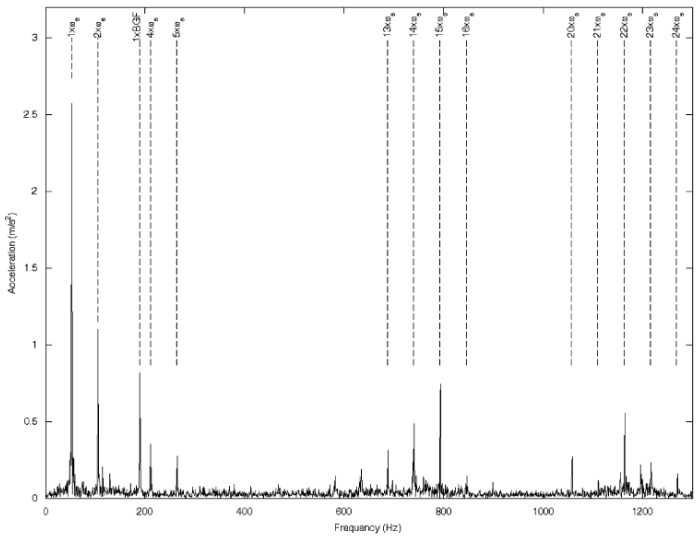

Figure 2.6. Vibration spectrum of a ball bearing after 130 hours of operation [31].

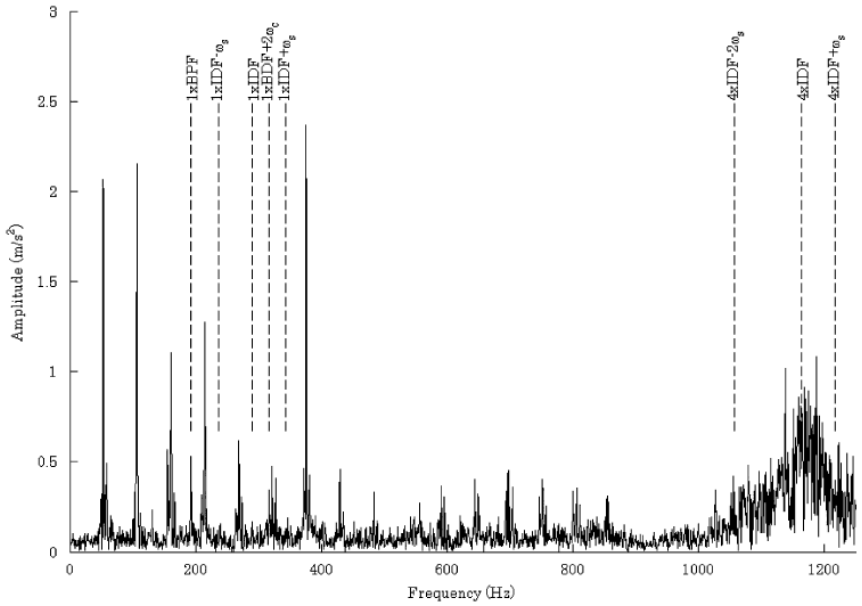

Figure 2.7. Vibration spectrum of a ball bearing after 980 hours of operation [31].

2.4 Feature in Time-Frequency Domain

By signal processing, it is aimed to obtain meaningful features from a signal by transforming it into an appropriate and informative form. Fourier transform is normally utilized for signal processing in frequency domain to obtain the frequencies that may exist in the signal. However, in Fourier based signal analysis, the method is not able to assign each frequency to the corresponding time.

It should be noted that the frequency behavior of a large number of engineering systems changes with time. Therefore a different method is required to analyze the signal measured from such systems. For such systems of time varying frequency content more effective methods such as Time-Frequency (TF) distributions are employed to represent the signal behavior. In a typical time-frequency analysis the time domain signal is mapped into another plane called time-frequency plane. This new transformation is a two-dimensional function of time and frequency. The goal of the time domain and frequency domain signal analysis is to obtain statistical and spectral features of the signal. One of the features that can be obtained is the signal energy. Assume

the time domain signal is represented by $x(t)$ and the representation of the signal in the frequency domain is shown by $x(f)$. One can define the energy of the signal per unit time, $|x(t)|^2$, as well as the energy of the signal per unit frequency $|x(f)|^2$ at any particular frequency by applying the Fourrier transform to the time domain signal $x(t)$. As it was discussed such analyses does not describe the specification of the signal when the frequency content of the signal changes with time or the frequency content of the signal exhibit random behavior.

Time-frequency distributions has several classes. They can be divided in two main category of the linear and bilinear or quadratic classes. The linear class contains wavelet transform and Short-Time Fourier transform (STFT) methods and the bilinear or quadratic category includes the Cohen's class and affine distributions. Of all of these classes of time-frequency distributions (TFD), the energy class of time-frequency distributions are normally used in practice. In these classes of TFDs the total energy of the signal at any specific time or frequency is usually of interest. These classes of the time-frequency distributions is also recognized as Cohen classes of TFDs in recognition of the contributions of Leon Cohen to this field [33]. There is a disadvantage associated with this classes of TFDs that they have cross terms or artifacts due to their bilinear property. Such artifacts are also known as ghosts effects. The effects are created when there are several frequency components in the spectrum of the signal [9, 33].

2.4.1 Wigner-Ville distribution

By performing a time-frequency analysis, a three-dimensional time, frequency and amplitude representation of the signal is obtained. Such representation is very suitable to demonstrate the transient events in the signal. The Wigner distribution [34] and its several forms has been used in the diagnostics of the faults in mechanical systems [35]. One can obtain the Wigner-Ville distribution for a non-stationary signal by generalizing the relation between the power spectrum

and autocorrelation function. This time-frequency distribution has found applications in different engineering disciplines such as signal processing of speech signals [36], biological signals [37], vibration [38] and acoustics [38] as well as on signals measured from building under earth-quake excitations [39]. The Wigner function [34] was first introduced in statistical mechanics by Wigner in 1932 and its application was extended to signal processing by Ville in 1948 [40] who proposed a new distribution called Wigner-Ville distribution. The Wigner-Ville distribution of a time-varying signal $x(t)$ can be obtained from the general form of the time-frequency distributions called Cohen class of distributions. The general class is defined as in equation 11 [33].

$$w(t,\omega) = \frac{1}{2\pi}\iiint e^{-j\theta - j\tau\omega - j\theta u}\ \emptyset(\theta,\tau)x\left(u+\frac{\tau}{2}\right)x^*\left(u-\frac{\tau}{2}\right)dud\tau d\theta \qquad (11)$$

where $x(u)$ is time representation of the signal. $\emptyset(\theta,\tau)$ is defined as the kernel of the time-frequency distribution. Several forms of the time-frequency distributions can be obtained by using different mathematical definition for the kernel of the general form of the time-frequency distribution. One can obtain the Wigner-Ville distribution by setting $\emptyset(\theta,\tau) = 1$ in the equation 11 [41]. The equation 11 is defined for continuous signals. However, in order to employ the Wigner-Vill distribution in practical applications, one should discretize the distribution. The Wigner-Ville distribution is a bilinear distribution and this characteristics is problematic since it generates frequency components that are not desirable. These components have been known as cross-terms, artifacts or spurious terms. These cross terms are larger in amplitude comparing to the spectral contents of the signals under investigation. Two of the methods that helps eliminating these cross terms is windowing the signal and smoothing the signal.

The Windowed Wigner-Ville distribution reduces the level of the artifacts and enhances the resolution property [42]. The reduction of the spurious terms is usually obtained by windowing and smoothing in both time and frequency domain. By applying two windows in both time and

frequency domains, another form of the Wigner-Ville distribution is obtained that is called smoothed-pseudo Wigner-Ville distribution (SPWVD) and defined by equation 12. [33, 41, 43, 44]. Although a better suppression of the artifacts is obtained, the frequency resolution is affected adversely. Equation 12 shows the SPWVD for a sampled signal of $x(n)$ [43, 44].

$$SPWVD_x(n,m) = \frac{2}{\Delta t} \sum_{p=-\frac{Q}{2}+1}^{\frac{Q}{2}-1} \sum_{k=-\frac{M}{2}+1}^{\frac{M}{2}} |h(k)|^2 x(n+k)x^*(n-k)\exp(-j2\pi mk/M)g(n-p) \qquad (12)$$

where Δt is measured in seconds, M and Q are the size of the frequency and time smoothing functions, respectively.

2.4.2 Feature extraction from the signal in time-frequency domain

After calculation of the time frequency representation of the signal, it is aimed to extract informative features from the time-frequency representation of the signal. Energy of the signal in time-frequency plane is the candidate for fault diagnosis purpose. To obtain the energy in either time domain or frequency domain the signal representation in the time-frequency plane should be integrated along each of the time or frequency variable. The integration is defined in equation (13) and (14) over time and frequency [43-45]. In the Eqs. 13 and 14, the ρ is time-frequency energy density.

$$\int_{-\infty}^{+\infty} \rho_x(t,v)dt = |X(v)|^2 \qquad (13)$$

$$\int_{-\infty}^{+\infty} \rho_x(t,v)dv = |X(t)|^2 \qquad (14)$$

In order to obtain the total energy of the signal in both time and frequency plane, a two-dimensional integration over time and frequency is needed. This integration is taken as follows in equation 15.

$$E = \int_{-\infty}^{+\infty} \int_{-\infty}^{+\infty} \rho_x(t,v)dtdv \qquad (15)$$

The energy content of the smoothed-pseudo Wigner-Ville distribution (SPWVD) is employed as a diagnosis feature. As the mechanical faults appear on the raceways of the ball bearing, the energy

of the measured vibration signal changes. The vibration signal is of complex spectrum and therefore the energy in a joint time-frequency plane is a suitable candidate for the fault diagnosis purpose. The time-frequency toolbox for Matlab [46] is used for obtaining the energy feature from smoothed pseudo Wigner-Ville distribution.

2.5 Approximate Entropy

Approximate entropy is a statistical measure that is used to quantify the complexity or regularity of time series. The approximate entropy was proposed by Pincus [47] in 1992. Its application was in the analysis of the Electroencephalography (EEG) signals [48], fatal heart rate [49] and other biological signal processing applications [50, 51]. The approximate entropy has a number of interesting properties that makes it suitable for signal processing applications in fault diagnosis of machinery. It is a robust estimate that can be obtained using in short data and it can be applied to both deterministic and stochastic signals [52]. Such characteristics makes it appropriate for the application of the experimentally measured signals that are of short duration and are often noisy [52]. In the following paragraphs the algorithm to calculate the approximate entropy is discussed. Also Figure 2.8 shows the different steps in calculating the approximate entropy.

Assume a signal is represented by a time-series of N points such as $x(n) = x(1), x(2), \dots, x(N)$. In addition to the N, there are two other parameters that should be assumed. m is the dimention of the vector formed from the original data and r is a threshold parameter. The steps toward calculation of the approximate entropy is as following [47, 52]:

1. Create the m-vectors $X(1) \dots X(N - m + 1)$ as defined below:

$$X(i) = [x(i), x(i + 1), \dots, x(i + m - 1)] \qquad i = 1, \dots, N - m + 1$$

2. Define the distance function between the formed vector, $X(i)$ and $X(j)$, as the maximum absolute distance between the two formed vectors.

$$d[X(i), X(j)] = \max_{k=0,m-1}[|x(i+k) - x(j+k)|] \qquad i = 1, N-m+1 \qquad (16)$$

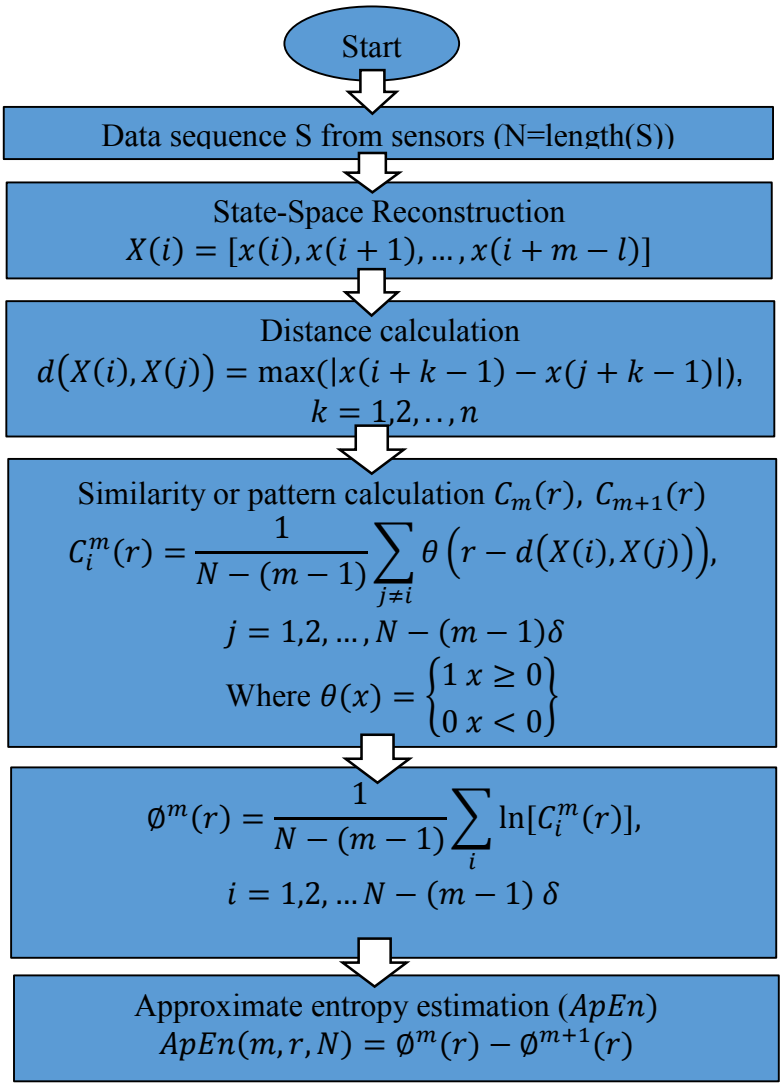

Figure 2.8. Steps toward calculation of the approximate entropy for a given time series [47, 53].

3. For each of the formed $X(i)$, calculate the number of distances, $d[X(i), X(j)]$ ($j = 1, N-m+1$), calculated in step 2 that is below the threshold value of r, then divide the obtained number to the total number of formed vectors ($N-m+1$)

Assume $N^m(i)$ =the number of $d[X(i), X(j)]$ that are smaller than r. Then, define $C_r^m = \frac{N^m(i)}{N-m+1}$.

Find $C_r^m(i)$ for all $i = 1, \dots, N-m+1$

4. Calculate the natural logarithm of each $C_r^m(i)$ and calculate the average over i as in equation 17.

$$\emptyset^m(r) = \frac{1}{N-(m-1)} \sum_i^{N-m+1} \ln[C_i^m(r)] \quad (17)$$

5. Increase the dimension of the formed vector to $m + 1$ and repeat the steps from 1 to 4 to find $C_r^{m+1}(i)$ and $\phi^{m+1}(r)$

6. Calculate the approximate entropy as in equation 18.

$$ApEn(m, r, N) = \emptyset^m(r) - \emptyset^{m+1}(r) \quad (18)$$

The equation 18 can be interpreted as the possibility of construction of new patterns in the time-series as the dimension m is increased to $m + 1$ [47, 49, 54]. The regularity or randomness of the signal can be determined by the approximate entropy measure. It can be said that the higher values of the approximate entropy is equivalent to the higher possibility of creation of the new pattern in the signal. For example if the signal under investigation is a periodic single frequency signal, then it is expected that the signal has a high regularity and such time-series is of lower approximate entropy. High regular signals can have an approximate entropy of values close to zero. The signals that have multiple frequency components in the spectrum, usually have less level of the regularity and this results in high values of approximate entropy. In this thesis a code is implemented for calculation of approximate entropy from vibration signals.

2.5 Shannon Entropy

Entropy is defined as a measure of the uncertainty of a random variable. The concept of the entropy first was introduced by Claude E. Shannon in 1948 [55-57] and is often referred as Shannon entropy. The Shannon entropy is in fact the expected value of the information content in bit of information. It is also equivalent to the average missing information when the value of the random variable is not known. Shannon used the probability theory to model the information sources.

Assume that a discrete random variable X has a probability distribution of the $D = [p_1, p_2, \dots, p_n]$, the Shannon entropy of the random variable is defined as:

$$S = P_i \sum_{i=1}^{n} \log \frac{1}{p_i} = -P_i \sum_{i=1}^{n} \log P_i \quad (19)$$

For the continuous systems the entropy function can be formulated as in equation 22 given the probability density function (PDF) of the random variable [58].

$$S = -\int PDF(x)\, log\big(PDF(x)\big)\, dx \quad (22)$$

In the definition of the Shannon entropy if the base of the logarithm is chosen as 2, the unit of the entropy is measured in *bits*. The base of the logarithm of *e* defines the unit of the entropy as *nats*. The term $\frac{1}{P_i}$ can be regarded from two points of view. First, it can be interpreted as the amount of uncertainty associated with the outcome. It can also be described as the amount of the information gained by knowing the outcome. The summation in the formula gives a statistical average of the amount of uncertainty or information. Entropy can also be seen as a measure of dispersion in the probability distribution of the random variable. Shannon entropy is employed in different applications such as in signal and image processing. Coifman *et al.* [59] employed Shannon entropy measure as a cost function in signal and image compression and provided a geometric interpretation for that. Kapur *et al.* [60] used the Shannon definition of the information entropy for thresholding of the histogram of the image. Sahoo *et al.* [61] also employed the information theory measures of entropy such Shannon entropy and Renyi entropy for thresholding and segmentation of the digital images. Albuquerque *et al.* [62] also used the Tsallis entropy for image thresholding purpose. In addition to the image thresholding application, Sabuncu [63] utilized Renyi entropy for image registration. Coifman also utilized the information entropy for the compression of the acoustic signals [64]. Various forms of information entropy, is used for determining the order of the time-series of physical measurements for instance a signal or an image to quantify their

information content. The first step in calculating the Shannon entropy is determining the probability distribution of the given random variable. This task can be done by calculation of the histogram of the observations. Several methods is available for the calculation of the histogram that includes linear and logarithmic binning of the data. Of the others methods to calculate the histogram of the data is the method based on cumulative distribution function that does not require binning.

Chapter 3. Experimental Quantification of the Vibration Features

3.1 Experimental Setup

In the previous chapter the features related to the fault diagnosis of ball bearings were introduced and defined theoretically. Now in this chapter, the experimental setup that is used to perform the experiments is introduced. The experimental data provided by department of Electrical Engineering at Case Western Reserve University is employed to perform the fault diagnosis analysis. The details of the experimental setup is explained below. Experiments are performed employing a 2 hp Reliance Electric motor, and the acceleration data is acquired at different locations that are both close to and far from the motor ball bearings.

The types of faults of the ball bearings in this research is formed artificially. The defects on the surface of the ball bearings are created using electro-discharge machining (EDM). The size of the diameter of the defects varies from 0.007 inches to 0.040 inches. The fault diameters of the ball bearings are 0.007, 0.014, 0.021, 0.028, and 0.040 inch. The location of the defects are on the inner raceway, balls and outer raceway. Once the faults are introduced in the ball bearings, the defective ball bearings are installed into the test motor and the data acquisition starts. The vibration data was acquired for four levels of the load that is labeled from 0 to 3 horsepower. The changes in the motor load results in variation of the speed of the motor and the obtained motor speed changes from 1797 to 1720 RPM.

The ball bearing fault diagnosis simulator is shown in Figure 3.1. The test rig's components includes of a 2 hp motor (left), a torque transducer and encoder (center), a dynamometer (right), and control electronics. The rotor shaft is supported by test bearings. Accelerometers are employed to measure the vibration data. They are connected to the ball bearings' housing using a magnetic attachment. The accelerometers are located at the 12 o'clock position of the housing.

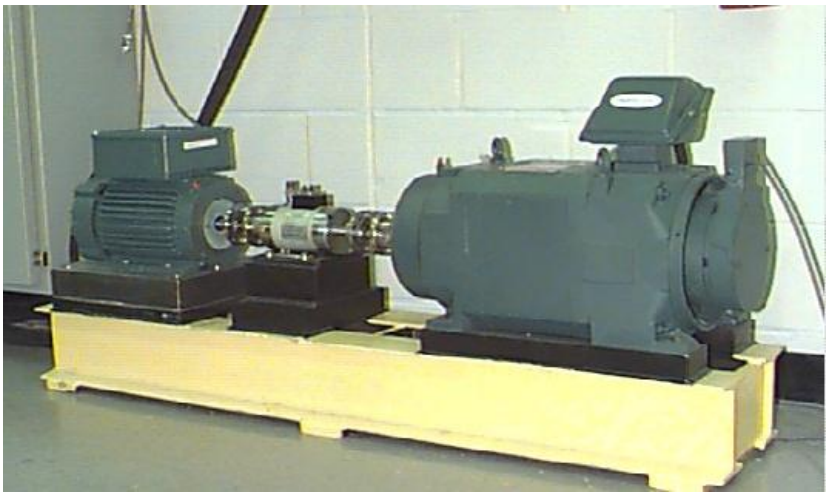

Figure 3.1. The ball bearing tester from Case Western Reserve University.

A 16 channel data acquisition unit is used to obtain the vibration signals and the recorded signals are post-processed in Matlab environment. The digital data was collected at 12,000 samples per second. Speed and horsepower data are measured using the torque transducer/encoder.

In this chapter, the inner race way fault is selected for investigations to calculate the feature space related to severity of the faults. Six features including RMS, Kurtosis, skewness, energy in the TFD plane, approximate entropy and Shannon entropy will be calculated for the case with inner race way fault. The features will be calculated in Matlab software.

3.2 Experimental Results

3.2.1 RMS results

One of the first ways to assess the level of the vibration level is to measure the root mean square (RMS) of the vibration signal at the housing. The technique should be applied on a range of the fault size. Figure 3.2, shows the RMS feature calculated from vibration signal of the faulty ball bearing for 16 experiments. The RMS value of the vibration signals is plotted versus each of the experiments with different fault size. The first four belongs to a ball bearing of 0.007 inch fault. For that specific level of fault size, the loading is increased from level 0 to 3.

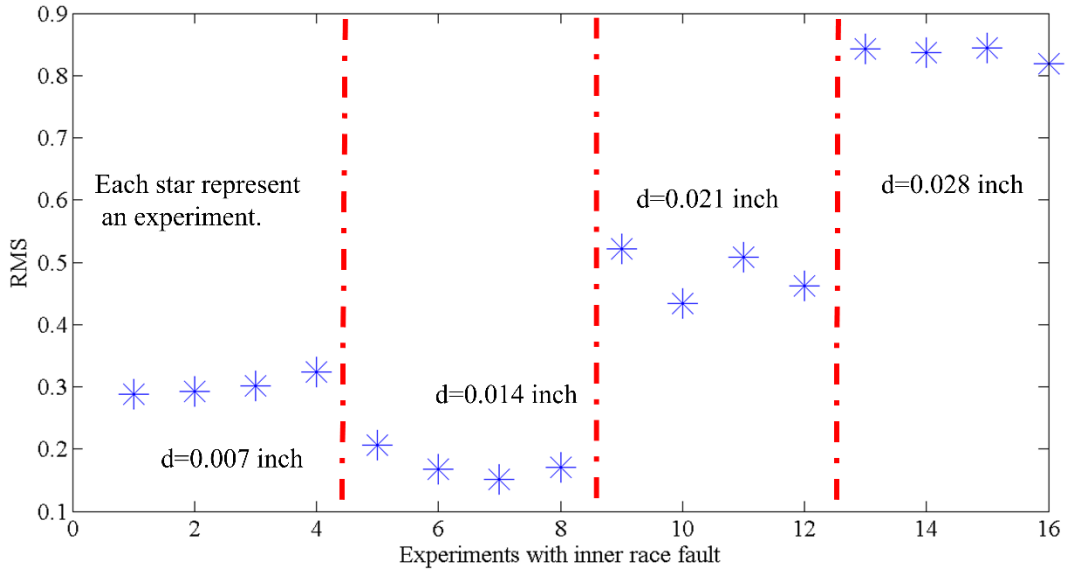

Figure 3.2. The RMS feature calculated for 16 experiments of different fault severity from 0.007 to 0.028 inch with 0.007 inch increment.

The increase in the loading results in the speed variation of 1797, 1772, 1750 and 1730 rpm. It can be observed that the RMS data related to the same classes of faults have somewhat similar level. It is observed that within the constant defect size, the RMS level does not change significantly for the change in the loading condition and its consequent speed variation. The vibration response of the ball bearing is more significant for the faults of higher severity and the RMS grows as the size of the fault grows. It is apparent that the RMS data can be well clustered in four groups. Each cluster represent the severity of the fault. It can be concluded that larger defect size increase the vibration level of the ball bearings. Consequently, as the vibration level is increased, the amplitudes of the recorded vibration signals attains a higher value of RMS.

3.2.2 The kurtosis results

A signal with a Gaussian distribution has a kurtosis value equivalent to 3. As the ball bearings degrades impulses appear in the time domain signal and consequently the distribution of the signal is changed. The signal of an impulsive behavior usually has a kurtosis value greater than the 3.

Figure 3.3 shows the kurtosis feature calculated from 16 experiments related to four classes of faults' severity. It can be observed that the kurtosis data is clustered well into four groups and each group of experiments has similar kurtosis values. The value of the kurtosis of the signals does not change with the changes in the load level and consequent speed level.

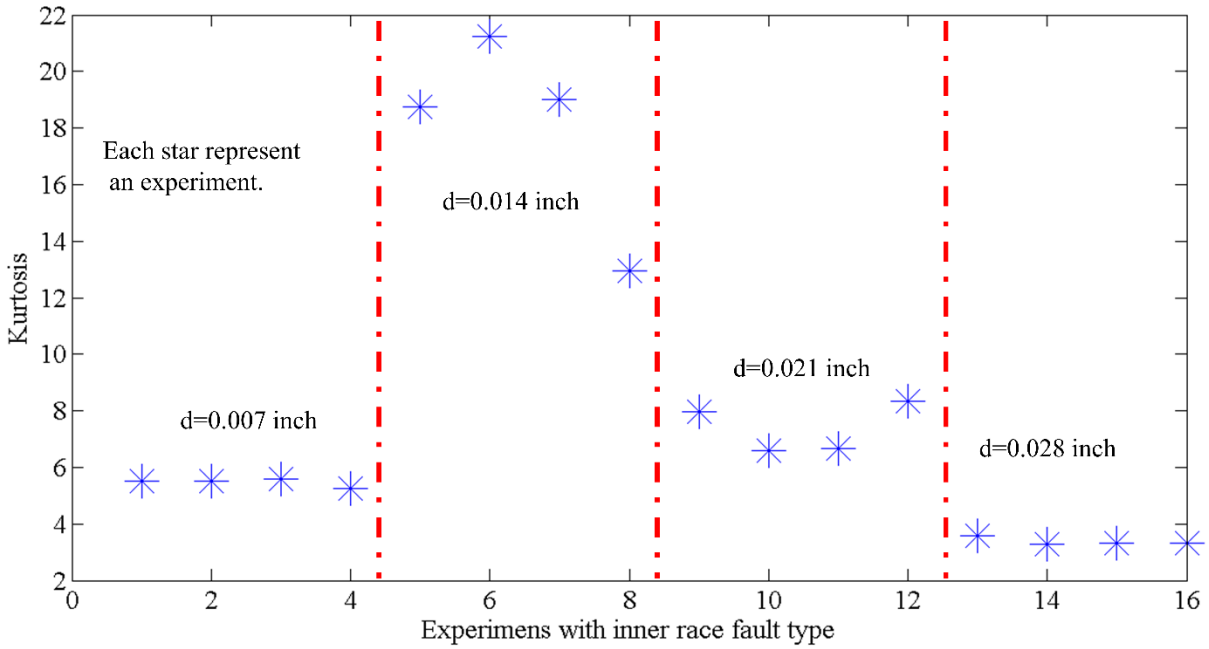

Figure 3.3. The kurtosis feature calculated for 16 experiments of different fault severity from 0.007 to 0.028 inch with 0.007 inch increment.

The value of kurtosis increases significantly as the severity of fault increases from 0.007 inch to 0.014. But as the fault severity increases from 0.014 inch to 0.021 and 0.028 inch, the kurtosis feature decreases. The increase in the value of the kurtosis as the fault size increases from the 0.007 inch to 0.014 inch can be interpreted as the increase of the impulsive oscillations and burst in the vibration signals. As the diameter of the defects increases, the impulsive behavior of the vibration signals are reduced and consequently the kurtosis parameter reduces again to the values similar to the defects of smaller size. Therefore, kurtosis feature cannot play a reliable role for fault diagnosis of the ball bearing. This result is in agreement with the results explained in [65].

3.2.3 The skewness results

The skewness of a time-series is a measure to quantify the lack of symmetry and it attains both positive and negative values. The skewness can characterize the level of the asymmetry of the probability distribution of the signal around its mean. If the signal is symmetric, then the skewness value is around zero. In fact, the negative skewness means that the statistical distribution is skewed to the left and the tail on the left hand side is longer than the tail on the right hand side and in this condition the mean is less than the mode. Once the right tail of the distribution is longer than its left tail, then the distribution is right skewed and in this condition the mean is greater than the mode. Such distribution result in positive skewness. Figure 3.4 shows the skewness feature calculated from 16 experiment related to four classes of faults.

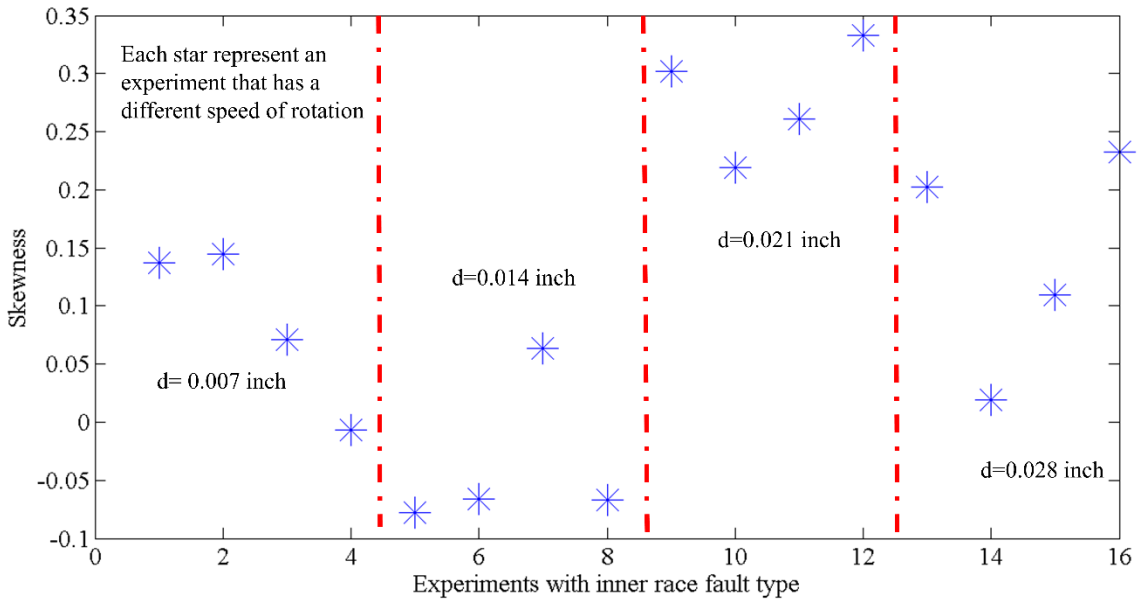

Figure 3.4. The skewness feature calculated for 16 experiments of different fault severity from 0.007 to 0.028 inch with 0.007 inch increment.

It can be observed that initially the skewness decreases as the severity of the faults increases from the 0.007 inch to 0.014 inch. The skewness feature attains negative values for the case with the diameter of 0.014. However, as the diameter of the faults increases, the value of the skewness

feature increases too. It is observed that the load variation, within a constant diameter of defect, also affects the skewness level. It can be concluded that for the low level of the faults, i.e. the small diameter of the defect and very large size defects the skewness is positive. Since the skewness feature does not provide a consistent trend, it cannot be used as a diagnosis feature space and its utilization requires expert level of interpretation.

3.3.4 The energy of signal in time-frequency domain

Non-stationary behavior of the vibration signals requires a time-frequency analysis for detection of the spikes in the signal. Therefore, the vibration signals are transformed into the time-frequency domain in order to identify the spikes in the signals. The defects in the raceways of the ball bearings induce a high instantaneous energy in the vibration signal.

These high energy spikes is reflected as a localized energy in time-frequency domain. Since the spectrum of the vibration signals are of multicomponent nature, once they are transformed into the time-frequency domain, the transformation creates artifacts and spurious terms. In order to reduce such cross-terms a smoothed pseudo Wigner-Ville distribution is employed for the time-frequency distribution.

Figure 3.5 shows the energy of vibration signal in time-frequency domain. As it is evident, the data related to 16 experiment are clustered very well. The data show an increasing behavior in tests of higher fault severity. It is revealed that the signals measured from the defective ball bearings with larger diameter are of higher energy in time-frequency domain. This makes the feature suitable for fault diagnosis purposes. It is also observed that the load variation and its consequent speed variation does not affect the energy of the signal in the time frequency domain. The benefit of this feature is that it contains the total energy of the signal in both time and frequency domains. As it can be seen the energy feature exhibits higher values in experiments of 0.021 and 0.028 inch

faults than those of the tests of 0.007 inch and 0.014 size faults. Such consistent trend in the energy level of the SPWV representation of the signal makes it an appropriate feature for fault identification.

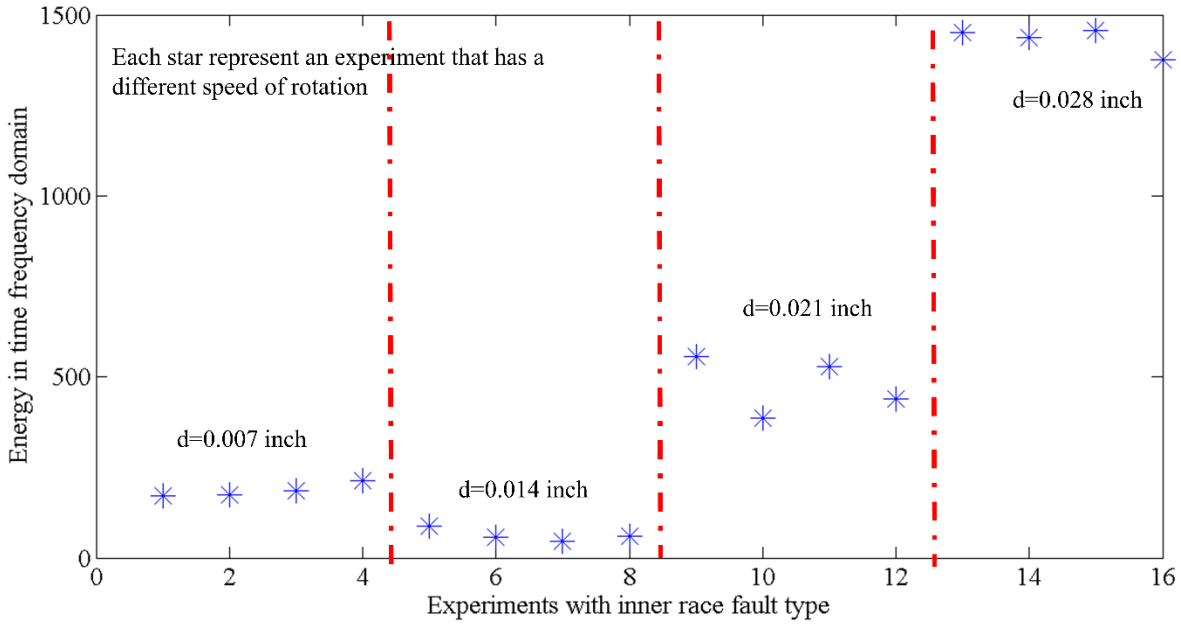

Figure 3.5. The Energy in time-frequency feature calculated for 16 experiments of different fault severity from 0.007 to 0.028 inch with 0.007 inch increment.

3.3.5 The Shannon entropy feature

In information theory, the entropy concept reveals the average amount of information in the data. The data could be a random variable in the form of a signal, a message, or a waveform. The entropy describes the amount of uncertainty associated with the random variable. The random variable is characterized by its probability distribution. The concept of the entropy was proposed by Shannon to quantify the density of information and to address this question that in a message to what extend the new character provides a new information.

Figure 3.6 shows the Shannon entropy feature calculated from 16 experiments. It can be observed that the data is clustered in four groups. Each groups belong to a class of fault severity. It is observed that the Shannon entropy has decreases as the severity of the defect increases from the

0.007 to 0.014 inches. The Shannon entropy is then employs an increasing trend with respect to the defect size.

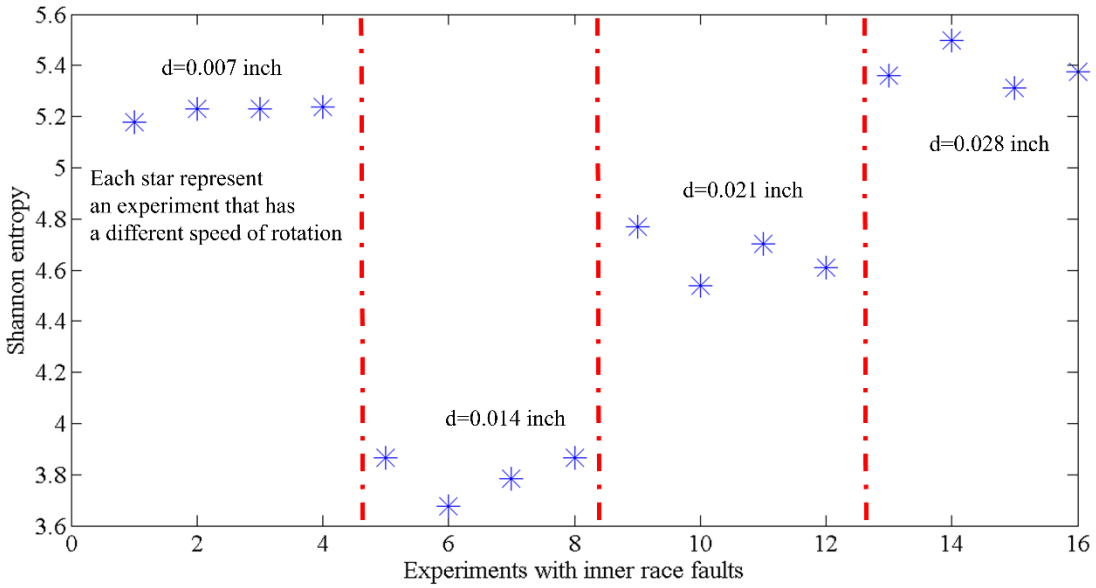

Figure 3.6. The Shannon entropy feature calculated for 16 experiments of different fault severity from 0.007 to 0.028 inch with 0.007 inch increment.

One can view the defective ball bearings as a dynamic system which is not deterministic and has stochastic behavior. The vibration signals could represent the description of the dynamics system and its evolution over time and the measured time-series represent all of the states of the system. From this point of view, high Shannon entropy means that in the measured time-series each new character provides new information. Low Shannon entropy confirms something that is already known [66]. The trend of the Shannon entropy makes it an appropriate feature for fault diagnosis of ball bearings.

3.3.6 The approximate entropy

Approximate entropy is a tool for investigation of the possibilities of forming new pattern within the time-series or measured signals and thus provides a measure for complexity or regularity of a

signal. Higher values of approximate entropy means higher possibility of formation a new pattern in the time-series [47, 49, 54].

Figure 3.7 shows the approximate entropy related to 16 experiments of different fault severity. It is observed that approximate entropy feature is clustered well to four classes of faults. The four classes of faults are 0.007, 0.014, 0.021 and 0.028 inch.

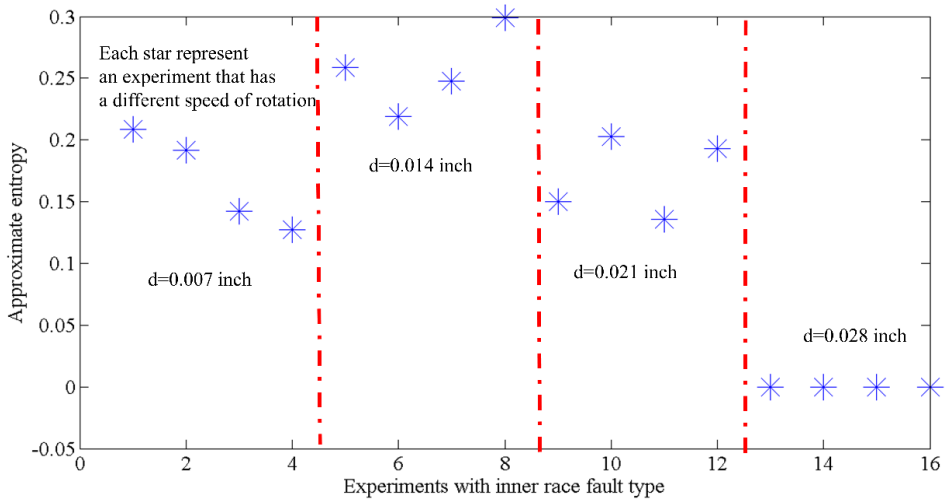

Figure 3.7. The approximate entropy feature calculated for 16 experiments of different fault severity from 0.007 to 0.028 inch with 0.007 inch increment.

A decreasing trend is observed as the severity of defects increases. It is observed that the least approximate entropy is obtained for the 0.028 inch class of fault. Approximate entropy shows the likelihood that similar patterns of observations will not be followed by additional similar observation [67]. A signal containing many repetitive patterns has a relatively small approximate entropy. It can be concluded that for the case of higher defect severity, the vibration signal contains more repetitive patterns.

3.3.7 The feature space for identifying the severity of the faults of ball bearings

After studying the trends of the 6 features for the condition monitoring purpose, three of the features were selected for the constructing of the feature space. The selected features are energy

in time-frequency domain, Shannon entropy and approximate entropy. These three features forms the basis of the diagnosis feature space for severity detection. Figure 3.8 shows the 3D feature space for severity detection of the inner race way faults. It can be observed that the selected feature space, can distinguish the classes of fault very well. The four classes of severity are clustered well in the 3D space.

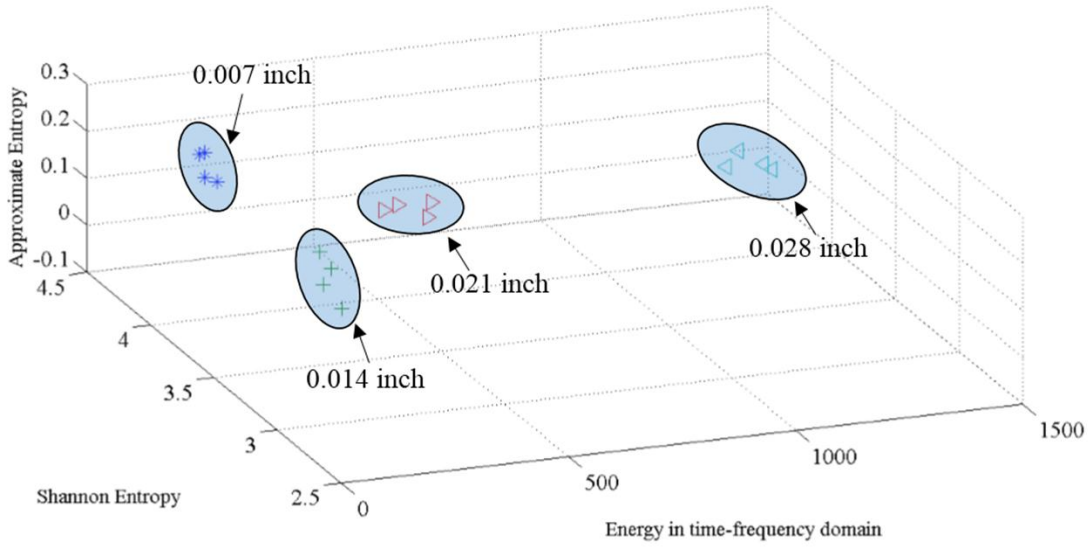

Figure 3.8. The reconstruction of feature space for severity detection based on energy in time-frequency, Shannon entropy and approximate entropy.

3.3.8 The feature space for classifying the faulty from healthy ball bearings

After building the feature space for severity detection, it is aimed to examine the proposed feature space for fault detection. For this aim, four other experiments related to healthy ball bearing are added to the feature space. The four new experiments belongs to healthy ball bearing with different loading condition with load levels 0 to 3. Figure 3.9 shows the new feature space and the normal case is depicted in purple circles. It is observed that feature space can distinguish all of the classes of faults properly. It is concluded that for the conditions tested, the feature space can cluster both severity of faults and also distinguish between the faulty and healthy bearings.

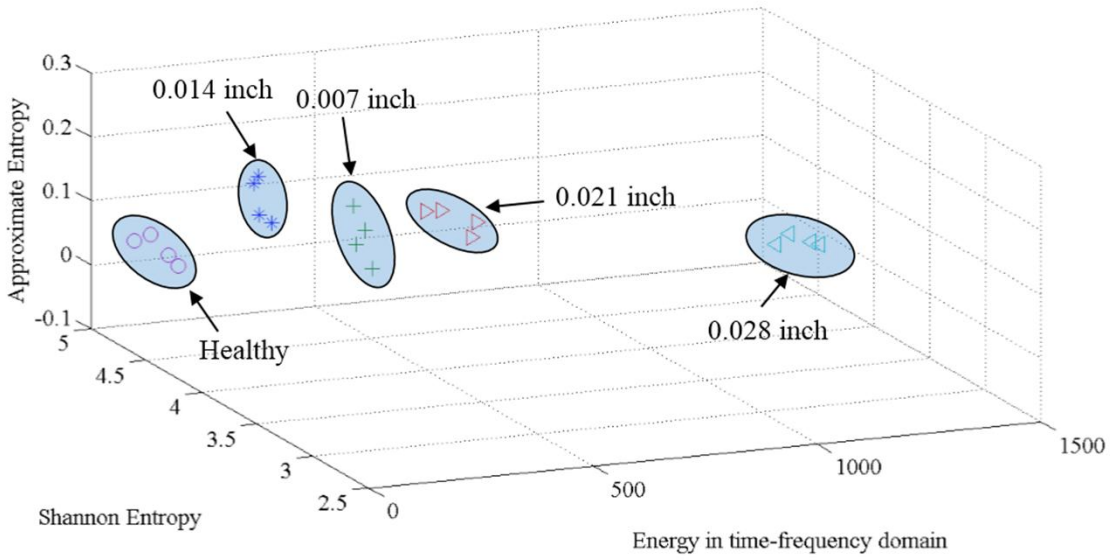

Figure 3.9. The diagnosis feature space including the case for healthy ball bearing.

Chapter 4. Conclusion

In this thesis a three dimensional feature space is identified for the purpose of fault diagnosis of ball bearings. This feature space contains energy in time-frequency plane, Shannon entropy and approximate entropy. Initially, 6 features were selected from the vibration signal of the ball bearings. Three features were identified as inappropriate for the classification purpose since the feature space was not well classified. The selected three features has this advantage that does not need the redundancy reduction module and also provide a good classification space for pattern recognition modules.

Two problem is investigated in this thesis. The first is to identify the severity of the faults and classification based on the severity. The second problem is about creating a good feature space for classification of the healthy ball bearings from the defective ball bearings. Result shows that the selected feature space is capable of clustering the faulty signals from the healthy signals. Additionally, it is capable of clustering different levels of severity of the faults. This provide a reliable three dimensional feature space for condition monitoring of ball bearings.

References

[1] Raison, B., Rostaing, G., Butscher, O., and Maroni, C. S., "Investigations of algorithms for bearing fault detection in induction drives," Proc. IECON 02 [Industrial Electronics Society, IEEE 2002 28th Annual Conference of the], pp. 1696-1701 vol.1692.

[2] Alewine, K., and Chen, W., 2010, "Wind Turbine Generator Failure Modes Analysis and Occurrence," Windpower 2010, Dallas, Texas, May 24-26, 2010.

[3] Harris, T. A., 2001, Rolling bearing analysis, Wiley.

[4] Heng, R. B. W., and Nor, M. J. M., 1998, "Statistical analysis of sound and vibration signals for monitoring rolling element bearing condition," Applied Acoustics, 53(1–3), pp. 211-226.

[5] Kar, C., and Mohanty, A. R., 2004, "Application of KS test in ball bearing fault diagnosis," Journal of Sound and Vibration, 269(1–2), pp. 439-454.

[6] Hall, L. D., and Mba, D., 2004, "Acoustic emissions diagnosis of rotor-stator rubs using the KS statistic," Mechanical Systems and Signal Processing, 18(4), pp. 849-868.

[7] Choi, Y.-C., and Kim, Y.-H., 2007, "Fault detection in a ball bearing system using minimum variance cepstrum," Measurement Science and Technology, 18(5), p. 1433.

[8] Qian, S., and Chen, D., 1993, "Discrete Gabor transform," Signal Processing, IEEE Transactions on, 41(7), pp. 2429-2438.

[9] Qian, S., and Chen, D., 1996, Joint time-frequency analysis: methods and applications, PTR Prentice Hall.

[10] Russell, P. C., Cosgrave, J., Tomtsis, D., Vourdas, A., Stergioulas, L., and Jones, G. R., 1998, "Extraction of information from acoustic vibration signals using Gabor transform type devices," Measurement Science and Technology, 9(8), p. 1282.

[11] Cocconcelli, M., Zimroz, R., Rubini, R., and Bartelmus, W., 2012, "STFT Based Approach for Ball Bearing Fault Detection in a Varying Speed Motor," Condition Monitoring of Machinery in Non-Stationary Operations, T. Fakhfakh, W. Bartelmus, F. Chaari, R. Zimroz, and M. Haddar, eds., Springer Berlin Heidelberg, pp. 41-50.

[12] Wang, W. J., and McFadden, P. D., 1996, "Application of wavelets to gearbox vibration signals for fault detection," Journal of Sound and Vibration, 192(5), pp. 927-939.

[13] Dalpiaz, G., Rivola, A., and Rubini, R., 2000, "Effectiveness and sensitivity of vibration processing techniques for local fault detection in gears," Mechanical Systems and Signal Processing, 14(3), pp. 387-412.

[14] Adewusi, S. A., and Al-Bedoor, B. O., 2001, "Wavelet analysis of vobration signals of an overhang rotor with a propagating transverse crack," Journal of Sound and Vibration, 246(5), pp. 777-793.

[15] Peng, Z. K., Chu, F. L., and Tse, P. W., 2005, "Detection of the rubbing-caused impacts for rotor–stator fault diagnosis using reassigned scalogram," Mechanical Systems and Signal Processing, 19(2), pp. 391-409.

[16] Chen, B. H., Wang, X. Z., Yang, S. H., and McGreavy, C., 1999, "Application of wavelets and neural networks to diagnostic system development, 1, feature extraction," Computers and Chemical Engineering, 23(7), pp. 899-906.

[17] Yen, G. G., and Kuo-Chung, L., "Conditional health monitoring using vibration signatures," Proc. Decision and Control, 1999. Proceedings of the 38th IEEE Conference on, pp. 4493-4498 vol.4495.

[18] Goumas, S., Zervakis, M., Pouliezos, A., and Stavrakakis, G. S., 2001, "Intelligent on-line quality control of washing machines using discrete wavelet analysis features and likelihood classification," Engineering Applications of Artificial Intelligence, 14(5), pp. 655-666.

[19] Mallat, S., and Hwang, W. L., 1992, "Singularity detection and processing with wavelets," Information Theory, IEEE Transactions on, 38(2), pp. 617-643.

[20] Sun, Q., and Tang, Y., 2002, "Singularity analysis using continous wavelet transfomr for bearing fault diagnosis," Mechanical Systems and Signal Processing, 16(6), pp. 1025-1041.

[21] Altmann, J., and Mathew, J., 2001, "Multiple band-pass autoregressive demodulation for rolling-element bearing fault diagnosis," Mechanical Systems and Signal Processing, 15(5), pp. 963-977.

[22] Lin, J., 2001, "Feature extraction of machine sound using wavelet and its application in fault diagnosis," NDT & E International, 34(1), pp. 25-30.

[23] Malhi, A., and Gao, R. X., 2004, "PCA-based feature selection scheme for machine defect classification," Instrumentation and Measurement, IEEE Transactions on, 53(6), pp. 1517-1525.

[24] He, Q., Kong, F., and Yan, R., 2007, "Subspace-based gearbox condition monitoring by kernel principal component analysis," Mechanical Systems and Signal Processing, 21(4), pp. 1755-1772.

[25] Akbaryan, F., and Bishnoi, P. R., 2001, "Fault Diagnosis of Single-Variate Systems Using a Wavelet-Based Pattern Recognition Technique," Industrial & Engineering Chemistry Research, 40(16), pp. 3612-3622.

[26] Ghate, V. N., and Dudul, S. V., 2010, "Optimal MLP neural network classifier for fault detection of three phase induction motor," Expert Systems with Applications, 37(4), pp. 3468-3481.

[27] Lei, Y., He, Z., and Zi, Y., 2009, "Application of an intelligent classification method to mechanical fault diagnosis," Expert Systems with Applications, 36(6), pp. 9941-9948.

[28] Lou, X., and Loparo, K. A., 2004, "Bearing fault diagnosis based on wavelet transform and fuzzy inference," Mechanical Systems and Signal Processing, 18(5), pp. 1077-1095.

[29] Mathew, J., and Alfredson, R. J., 1984, "The Condition Monitoring of Rolling Element Bearings Using Vibration Analysis," Journal of Vibration and Acoustics, 106(3), pp. 447-453.

[30] Swansson, N. S., and Favaloro, S., 1984, "Applications of vibration analysis to the condition monitoring of rolling element bearings."

[31] Karacay, T., and Akturk, N., 2009, "Experimental diagnostics of ball bearings using statistical and spectral methods," Tribology International, 42(6), pp. 836-843.

[32] Nandi, S., Toliyat, H. A., and Xiaodong, L., 2005, "Condition monitoring and fault diagnosis of electrical motors-a review," Energy Conversion, IEEE Transactions on, 20(4), pp. 719-729.

[33] Cohen, L., 1989, "Time-frequency distributions-a review," Proceedings of the IEEE, 77(7), pp. 941-981.

[34] Wigner, E., 1932, "On the Quantum Correction For Thermodynamic Equilibrium," Physical Review, 40(5), p. 749.

[35] Meng, Q., and Qu, L., 1991, "Rotating machinery fault diagnosis using Wigner distribution," Mechanical Systems and Signal Processing, 5(3), pp. 155-166.

[36] Boashash, B., and Abeysekera, S. S., "Two Dimensional Processing Of Speech And Ecg Signals Using The Wigner-Ville Distribution," pp. 142-153.

[37] Novak, P., and Novak, V., 1993, "Time/frequency mapping of the heart rate, blood pressure and respiratory signals," Med. Biol. Eng. Comput., 31(2), pp. 103-110.

[38] Baydar, N., and Ball, A., 2001, "A comparative study of acoustic and vibration signals in detection of gear failures using Wigner-Ville distribution," Mechanical Systems and Signal Processing, 15(6), pp. 1091-1107.

[39] Li, Y., and Zheng, X., 2007, "Wigner-Ville distribution and its application in seismic attenuation estimation," Appl. Geophys., 4(4), pp. 245-254.

[40] Ville, J., 1948, "Theorie et applications de la notion de signal analytique," Cables Transm., 2A(1), pp. 61–74.

[41] Claasen, T. A. C. M., and Mecklenbrauker, W. F. G., 1980, "The Wigner Distribution - a Tool for Time-Frequency Signal Analysis .3. Relations with Other Time-Frequency Signal Transformations," Philips Journal of Research, **35**(6), pp. 372-389.

[42] Boashash, B., 2003, Time Frequency Analysis, Elsevier Science.

[43] Flandrin, P., 1984, "Some features of time-frequency representations of multi component signals," Proceeding of IEEE Int. Conf. Acoustics, Speech, and Signal Processing, **3,**, pp. 41B.44.41-41B.44.44.

[44] Flandrin, P., and Goncalvès, P., 1996, "Geometry of Affine Time–Frequency Distributions," Applied and Computational Harmonic Analysis, 3(1), pp. 10-39.

[45] 1998, "Parametric homogeneity and non-classical self-similarity. II. Some applications," Acta Mechanica, 131(1-2), p. 47.

[46] Auger, F., Flandrin P., Goncalves P., and Lemoine O., , 1998, "Time–frequency toolbox," Centre national de la recherché scientifique, France, and Rice University, Houston, Tex., U.S.A.."

[47] Pincus, S. M., 1991, "Approximate entropy as a measure of system complexity," Proceedings of the National Academy of Sciences, 88(6), pp. 2297-2301.

[48] Ocak, H., 2009, "Automatic detection of epileptic seizures in EEG using discrete wavelet transform and approximate entropy," Expert Systems with Applications, 36(2, Part 1), pp. 2027-2036.

[49] Pincus, S. M., and Viscarello, R. R., 1992, "Approximate entropy: a regularity measure for fetal heart rate analysis," Obstetrics and gynecology, 79(2), pp. 249-255.

[50] Gu, Q., Ding, Y.-S., and Zhang, T.-L., 2010, "Prediction of G-Protein-Coupled Receptor Classes in Low Homology Using Chou's Pseudo Amino Acid Composition with Approximate Entropy and Hydrophobicity Patterns," Protein and Peptide Letters, 17(5), pp. 559-567.

[51] Guo, L., Rivero, D., and Pazos, A., 2010, "Epileptic seizure detection using multiwavelet transform based approximate entropy and artificial neural networks," Journal of Neuroscience Methods, 193(1), pp. 156-163.

[52] Fusheng, Y., Bo, H., and Qingyu, T., 2000, "Approximate Entropy and Its Application to Biosignal Analysis," Nonlinear Biomedical Signal Processing, John Wiley & Sons, Inc., pp. 72-91.

[53] Yan, R., and Gao, R. X., 2007, "Approximate Entropy as a diagnostic tool for machine health monitoring," Mechanical Systems and Signal Processing, 21(2), pp. 824-839.

[54] Pincus, S., 1995, "Approximate entropy (ApEn) as a complexity measure," Chaos: An Interdisciplinary Journal of Nonlinear Science, 5(1), pp. 110-117.

[55] Shannon, C. E., and Weaver, W., 1948, "A mathematical theory of communication," pp. 623-423.

[56] Hirschman, I. I., Jr., 1957, "A Note on Entropy," American Journal of Mathematics, 79(1), pp. 152-156.

[57] Shannon, C. E., 2001, "A mathematical theory of communication," SIGMOBILE Mob. Comput. Commun. Rev., 5(1), pp. 3-55.

[58] Rossing, T. D., 2007, Springer handbook of acoustics, Springer.

[59] Coifman, R. R., and Wickerhauser, M. V., 1992, "Entropy-based algorithms for best basis selection," Information Theory, IEEE Transactions on, 38(2), pp. 713-718.

[60] Kapur, J. N., Sahoo, P. K., and Wong, A. K. C., 1985, "A new method for gray-level picture thresholding using the entropy of the histogram," Computer Vision, Graphics, and Image Processing, 29(3), pp. 273-285.

[61] Sahoo, P., Wilkins, C., and Yeager, J., 1997, "Threshold selection using Renyi's entropy," Pattern Recognition, 30(1), pp. 71-84.

[62] Portes de Albuquerque, M., Esquef, I. A., Gesualdi Mello, A. R., and Portes de Albuquerque, M., 2004, "Image thresholding using Tsallis entropy," Pattern Recognition Letters, 25(9), pp. 1059-1065.

[63] Sabuncu, M. R., 2006, "Entropy-based image registration," Princeton University.

[64] Coifman, R., Meyer, Y., Quake, S., and Wickerhauser, M. V., 1994, "Signal processing and compression with wavelet packets," Wavelets and Their Applications, J. S. Byrnes, J. Byrnes, K. Hargreaves, and K. Berry, eds., Springer Netherlands, pp. 363-379.

[65] Tandon, N., and Choudhury, A., 1999, "A review of vibration and acoustic measurement methods for the detection of defects in rolling element bearings," Tribology International, 32(8), pp. 469-480.

[66] Sinai, Y. G., "www.abelprize.no/c61094/binfil/download.php?tid=61211."

[67] Ho, K. K., Moody, G. B., Peng, C. K., Mietus, J. E., Larson, M. G., Levy, D., and Goldberger, A. L., 1997, "Predicting survival in heart failure case and control subjects by use of fully automated methods for deriving nonlinear and conventional indices of heart rate dynamics," Circulation, 96(3), pp. 842-848.

Vita

Ali Kahirdeh was born in Tehran, Iran. He obtained his high school diploma in Physics and Mathematics from Kamal high school in 2000. He obtained his BSc. in Mechanical Engineering from Isfahan University of Technology in 2005. He also obtained his MSc. in Mechanical Engineering from Iran University of Science and Technology in 2007. He joined the Ph.D. program of Mechanical Engineering at Louisiana State University in 2008. He is also a MSc. candidate in the department of Electrical Engineering at Louisiana State University. He is expected to receive his Ph.D. degree in Mechanical Engineering and MSc. degree in Electrical Engineering in December 2014.